Frontiers in Bioscience Landmark

Front. Biosci. (Landmark Ed) **2026**; 31(8): 50478
https://doi.org/10.31083/FBL50478

Original Research

Plasma Extracellular Vesicle Profiles After Heart Transplantation are Associated With the Type of Allograft Rejection

Arthur Aquino[1], Lubov Korneva[1], Maria Osipova[1], Maria Bortsova[1], Maria Simonenko[1], Darina Sambur[1], Ivan Golovkin[1,2], Igor Kudryavtsev[1,3], Ekaterina Zaikova[1], Anna Kostareva[1], Olga Kalinina[1], Petr Fedotov[1], Alexey Golovkin[1,*]

[1]Institute of Molecular Biology and Genetics, Almazov National Medical Research Centre, 197341 St. Petersburg, Russia
[2]Center for Artificial Intelligence in Chemistry, ITMO University, 191002 St. Petersburg, Russia
[3]Department of immunology, Institute of Experimental Medicine, 197022 St. Petersburg, Russia
*Correspondence: golovkin_a@mail.ru (Alexey Golovkin)
Academic Editor: Natascia Tiso
Submitted: 28 January 2026 Revised: 23 March 2026 Accepted: 2 April 2026 Published: 3 August 2026

Abstract

Background: Heart transplantation (HT) remains the primary treatment for end-stage heart failure, but graft rejection—including acute cellular rejection (ACR), antibody-mediated rejection (AMR), and chronic rejection such as cardiac allograft vasculopathy (CAV)—significantly impacts long-term patient outcomes. This study investigates the role of circulating plasma extracellular vesicle profiles as potential biomarkers for distinguishing between different rejection types following HT. **Methods**: We enrolled 85 HT patients with post-transplant follow-up ranging from 2 to 140 months. The cohort included patients diagnosed with AMR (n = 23), ACR (n = 11), CAV (n = 20), and those without rejection (R0, n = 31). Extracellular vesicle profiles were analyzed using the MACSPlex Exosome Kit, and associated cytokine profiles were assessed using the MILLIPLEX Human Cytokine Panel A. Statistical analysis involved the Kruskal Wallis test followed by Dunn's post-hoc test for multiple comparisons and discriminant analysis. **Results**: Circulating plasma extracellular vesicle profiles demonstrated significant differences across post-transplantation time strata and varied according to the type of transplant rejection. During the first year post-HT, the main discriminant factors were extracellular vesicles (EVs) characterized by tetraspanins (CD9+, CD63+) and platelet markers (CD62P+, CD42a+). Five years post-transplantation, significant differences emerged in patients with AMR and ACR (both compared to each other and to the CAV/R0 groups). This difference corresponded with an increase in EV markers associated with immune cell activity (CD3+, CD4+, CD49e+, CD86+, CD20+, CD14+, CD209+, CD1c+, CD29+). Levels of prominent EV subpopulations correlated with IL-22 in CAV patients, whereas in AMR patients, they correlated with IL-17 and IL-25. **Conclusions**: These findings support the hypothesis that extracellular vesicles may participate in both direct and indirect antigen presentation and in the regulation of immune responses leading to allograft rejection after HT. Plasma extracellular vesicle profiles hold promise as non-invasive biomarkers for monitoring and differentiating rejection types in heart transplant recipients.

Keywords: heart transplantation; exosomes; extracellular vesicles; graft rejection; allografts; biomarkers; heart failure; tetraspanins

1. Introduction

End-stage heart failure is ultimately treated by heart transplantation (HT), which remains the only effective option for many patients and is included in international guidelines for the management of chronic heart failure [1]. More than 5500 heart transplants are performed worldwide each year, while the number of patients on transplant waiting lists continues to grow [2].

Improvements in immunosuppressive regimens and optimized post-transplant management have significantly increased recipient survival [3]. Nevertheless, graft rejection remains an important cause of morbidity and mortality. During the first three years after transplantation, fatal episodes of acute rejection account for approximately 3.9–9.8% of deaths; their incidence declines over time and falls to below 1% beyond ten years post-transplant [3]. By contrast, chronic graft injury—most notably cardiac allograft vasculopathy (CAV), a form of chronic rejection—becomes more prevalent in the long term, affecting about 3.2% of patients in the first year and rising to roughly 12.5% subsequently. Overall, graft dysfunction accounts for 17–26% of deaths from 30 days up to 15 years after transplantation [3].

CAV is an immune-mediated pathological remodeling of the coronary vasculature in the transplanted heart. In response to injury, the vessel wall undergoes concentric intimal hyperplasia and fibrosis, resulting in altered wall thickness, reduced luminal diameter and changes in vessel circumference; these lesions differ morphologically and distributionally from atherosclerotic plaques [4]. Immune mechanisms are central to CAV pathogenesis: graft alloantigens (HLA class I and II) expressed on endothelial cells trigger host T- and B-cell responses. Activated

T-cell subsets produce key cytokines—notably IFN-γ and TGF-β—that drive both cellular and humoral components of the response in CAV [4,5]. Donor-specific antibodies (DSA) have also been implicated as active mediators of arterial injury in CAV [6].

Transplant rejection occurs as either acute cellular rejection (ACR) or antibody-mediated rejection (AMR). ACR is driven primarily by donor-reactive T lymphocytes: CD4+ helper and CD8+ cytotoxic T cells are activated against donor antigens, with effector CD8+ T cells acting as principal mediators of graft destruction [7,8]. Central to T-cell-mediated alloimmunity is antigen presentation in the context of major histocompatibility complex (MHC) molecules. Antigen presentation can occur via the direct pathway, in which donor antigen-presenting cells (APCs) display donor MHC–peptide complexes to recipient T cells, or via the indirect pathway, where recipient dendritic cells process donor antigens and present derived peptides on recipient MHC molecules. A semi-direct pathway has also been described, whereby recipient APCs acquire intact donor MHC–peptide complexes and activate T cells, a process that can be facilitated by EVs and exosomes [9].

EVs are membrane-bound nanoparticles naturally released by cells, serving as key mediators of intercellular communication by transferring diverse biomolecules, including RNA, DNA, proteins, lipids, metabolites, and cytokines [10,11]. Found in various biological fluids (e.g., blood, urine, saliva, cerebrospinal fluid), they underscore systemic relevance [12,13]. Donor-derived EVs carrying MHC molecules are capable of "cross-dressing" host APCs and thereby initiating semi-direct alloimmune responses [14,15,16,17]. Importantly, EVs can exit the graft before it is fully vascularized, providing a mechanism for initiating immune activation at very early stages after transplantation. Unlike donor APCs, which generally require vascular access to enter the systemic circulation, EVs have the potential to act from the outset and may therefore serve as early drivers of graft injury [14,18].

Antibody-mediated rejection may arise from preexisting memory B cells in sensitized recipients or from *de novo* production of donor-specific antibodies (DSA) in nonsensitized patients [19]. B cells thus contribute to graft rejection through both cellular and humoral mechanisms. In the indirect pathway of alloantigen presentation, primed CD4+ helper T cells recognize donor-derived peptides presented by MHC class II molecules expressed on B cells, promoting B-cell activation and antibody production [20]. B-cell-derived EVs can also participate in these processes: they are capable of carrying MHC class II and associated antigens that may contribute to antigen presentation [21], and they frequently express co-stimulatory molecules such as CD86 as well as tetraspanins (CD37, CD53, CD63, CD81 and CD82), features that underscore their immunomodulatory potential [22].

Thus, rejection and CAV remain priorities for research into pathogenesis and for the development of rapid, non-invasive diagnostic approaches. In this context, EVs are increasingly considered potential regulators of alloimmune responses and promising biomarkers for liquid-biopsy-based detection of rejection.

2. Materials and Methods

Eighty-five samples from patients who underwent HT between January 2012 and December 2024 were included in the study (57 men and 28 women). These dates in the manuscript refer to the dates of the HTs (i.e., the dates when the patients underwent HT), not to the dates of sample collection. Ethical approval for collection and analysis of samples was granted by the Institutional Ethics Committee of V.A. Almazov National Medical Research Centre, protocol no. №4101-22, dated 24 January 2022. All biological samples used in this study were collected after this approval date. Therefore, no samples were collected prior to 24 January 2022, and no separate prior ethical approval was required. All enrolled patients provided written informed consent. At each visit, patients underwent a clinical evaluation, routine biochemical tests, endomyocardial biopsy (EMB), and blood sampling. The blood was collected immediately before the biopsy to exclude procedure-related artifacts.

Heart transplant rejection was diagnosed through morphological examination of endomyocardial biopsy (EMB) using the current grading criteria of the International Society for Heart and Lung Transplantation (ISHLT). Twenty-three patients were diagnosed with AMR (AMR II and AMR III), 11 with ACR (grade R2 and grade R3), 20 with CAV (CAV2, CAV3), and 31 without signs of rejection (R0, R1). Thus, the post-transplantation duration in patients included in the study was from 2 to 140 months. The distribution of patients according to transplantation duration is presented in Table 1.

All patients underwent induction of immunosuppression with basiliximab at the time of transplantation. During the first year, heart recipients received triple immunosuppressive therapy: calcineurin inhibitors (tacrolimus), mycophenolic acid, and glucocorticosteroids (GCS). Following HT, patients underwent a planned reduction in immunosuppressive therapy over the first year, according to the regimen (withdrawal of GCS and reduction in calcineurin inhibitor concentrations). Prophylactic medications were also discontinued: antiviral (valganciclovir, discontinued at 12 months post-HT), antifungal (nystatin, discontinued within 2 weeks post-HT), and antibacterial (sulfamethoxazole + trimethoprim for Pneumocystis carinii prophylaxis, discontinued at 6 months post-HT). After one year post-transplantation, maintenance therapy included calcineurin inhibitors (tacrolimus) and mycophenolic acid or mTOR inhibitors (everolimus). Glucocorticosteroid therapy was administered to treat rejection crises. There were no dif-

Table 1. Distribution of patients by type of heart transplant rejection and post-transplantation duration.

Group	Months post-transplantation Median (Q1; Q3)	AMR	ACR	CAV	R0
<1 year	5 (2; 7)	7	2	0	10
1–5 years	31 (21; 40)	11	6	8	10
>5 years	84 (76; 108)	5	3	12	11

AMR, antibody-mediated rejection; ACR, acute cellular rejection; CAV, cardiac allograft vasculopathy; R0, without rejection.

Table 2. Characteristics of heart transplant recipients, Median (Q1; Q3).

	AMR	ACR	CAV	R0	*p*
Hemoglobin, g/L	130 (110; 154.5)	136 (107; 138)	129 (123; 145)	133 (124; 141)	
RBC, $\times 10^{12}$/L	4.59 (4.21; 5.05)	4.66 (3.59; 5.81)	4.74 (4.41; 5.01)	4.70 (4.28; 4.87)	
Hematocrit	37.9 (32.5; 43.8)	40.3 (31.3; 43.1)	39.3 (37.2; 41.2)	39.0 (35.6; 41.8)	
Platelets, $\times 10^9$/L	211 (166; 243)	241 (215; 336)	212 (146; 248)	217 (192; 237)	
WBC, $\times 10^9$/L	8.0 (4.4; 9.5)	7.1 (6.3; 7.6)	6.6 (5.1; 7.4)	6.2 (4.2; 8.8)	
Lymphocytes, $\times 10^9$/L	1.31 (0.97; 2.21)	1.78 (0.88; 2.28)	1.86 (0.97; 2.18)	1.76 (1.22; 2.16)	
Monocytes, $\times 10^9$/L	0.63 (0.38; 0.79)	0.76 (0.38; 0.78)	0.61 (0.52; 0.74)	0.56 (0.35; 0.71)	
Eosinophils, $\times 10^9$/L	0.07 (0; 0.16)	0.26 (0.06; 0.38)	0.05 (0; 0.14)	0.08 (0.02; 0.15)	
					$p1,2 < 0.01$
C-reactive protein, mg/L	8.4 (4.3; 39.8)	3.0 (1.3; 4.6)	3.5 (2.1; 6.7)	2.6 (1.3; 3.0)	$p1,3 < 0.01$
					$p1,4 < 0.01$
					$p1,2 < 0.01$
Creatinine, µmol/L	95.8 (75.6; 110.5)	181.0 (89.6; 235.9)	107.1 (85.2; 141.4)	85.7 (73.7; 116.5)	$p2,3 < 0.01$
					$p2,4 < 0.01$
Glucose, mmol/L	6.1 (5.1; 7.6)	6.1 (5.9; 7.2)	5.4 (5.0; 6.8)	5.5 (4.8; 6.2)	
Triglycerides, mmol/L	2.0 (1.4; 2.4)	1.3 (0.9; 1.7)	1.4 (1.0; 2.0)	1.3 (1.2; 1.6)	
Cholesterol, mmol/L	4.8 (4.0; 5.2)	4.0 (3.9; 4.0)	4.4 (3.6; 4.6)	3.8 (3.6; 4.7)	
HDL, mmol/L	1.31 (1.12; 1.54)	1.25 (1.11; 1.39)	1.14 (0.92; 1.46)	1.26 (0.96; 1.78)	
LDL, mmol/L	2.29 (2.09; 2.87)	2.13 (2.03; 2.45)	2.21 (1.80; 2.74)	2.10 (1.67; 2.60)	
VLDL, mmol/L	0.76 (0.65; 1.08)	0.58 (0.40; 0.77)	0.66 (0.46; 0.93)	0.59 (0.55; 0.74)	
Atherogenicity index	2.7 (1.9; 3.9)	2.2 (1.8; 2.6)	2.7 (1.4; 3.4)	2.1 (1.7; 3.0)	

WBC, white blood cells; HDL, high density lipoproteins; LDL, low density lipoproteins; VLDL, very low density lipoproteins.

ferences in the therapy administered between the groups (**Supplementary Table 1**).

The median age in the AMR group was 55 (43; 59) years, in the ACR group 50 (38; 60) years, in the CAV group 60.5 (48; 64.5) years, and in the R0 group 51 (44; 64) years. Diabetes mellitus was present as a comorbidity in 5 (22%) of the AMR patients, 1 (9%) of the ACR patients, 10 (50%) of the CAV patients, and 6 (19%) of the R0 patients. The laboratory characteristics of the patients are presented in Table 2. Patients with ACR had a higher level of CRP than patients in all other groups. Furthermore, the creatinine level in patients with ACR was higher than in patients in all other groups.

2.1 Extracellular Vesicles

Plasma was isolated from whole blood collected in K_3EDTA vacuum tubes. To prevent residual cellular contamination, each sample was processed by sequential centrifugation, as was previously shown by our group [23,24,25]. First, the blood tubes were centrifuged twice successively at 1500 ×g for 10 min at +18 °C, followed by one centrifugation at 3000 ×g for 20 min at +4 °C. After each centrifugation step, the supernatant was carefully transferred to a new conical tube. The resulting plasma was aliquoted and stored at –80 °C until further use. Plasma-derived EVs were analyzed using the MACSPlex Exosome Kit IO, human (cat. 130-108-813) (Miltenyi Biotec, Gaithersburg, MD, USA), following the manufacturer's instructions. Briefly, plasma samples were thawed and centrifuged at 3000 g for 10 minutes at +4 °C to remove any debris. All collected plasma samples were thawed and analyzed in a single batch to minimize technical variability. The clarified plasma was then diluted 1:2 (40 µL plasma + 80 µL sample dilution buffer) and incubated with 15 µL of MACSPlex EV capture beads. The resulting mixture was transferred to the wells of a 96-well filter plate and incubated overnight in the dark at room temperature on a plate shaker (450 rpm).

Following incubation, each well was washed with 200 µL of wash buffer. The buffer was then removed by vacuum filtration using a vacuum manifold, retaining the capture beads with bound EVs. Next, 135 µL of wash buffer

and 15 µL of the detection antibody cocktail (containing antibodies against CD9, CD63, and CD81) were added to each well. The plate was incubated for 1 hour in the dark at room temperature on a plate shaker.

After incubation, each well was washed again with 200 µL of wash buffer, and the buffer was removed by vacuum filtration as described above. A final wash step was performed by adding 200 µL of wash buffer to each well, incubating for 15 minutes in the dark at room temperature on a plate shaker, and then removing the liquid by vacuum filtration. Finally, 150 µL of wash buffer was added to each well, and the plate was transferred to the autosampler of a CytoFLEX S (Beckman Coulter, West Sacramento, CA, USA) flow cytometer.

Instrument settings and flow cytometry acquisition were performed according to the manufacturer's recommendations. The cytometry protocol was configured as follows: Three two-parameter dot plots were created: (1) Forward scatter (FSC) vs. side scatter (SSC); (2) Fluorescein isothiocyanate (FITC) vs. phycoerythrin (PE); and (3) PE vs. allophycocyanin (APC). The first plot (FSC vs. SSC) was used to gate on the capture beads. The second plot (FITC vs. PE) was used to define 39 distinct gates of beads positive for the corresponding EV marker. The third plot (PE vs. APC) was used to assess the fluorescence signal from each gated population of beads, indicating the presence and level of the specified marker on EVs within that population. For each EV population, we calculated the median of the mean intensity fluorescence (MIF) as measured in the APC channel. The panel of investigated EV markers is presented in **Supplementary Table 2**.

2.2 Nanoparticle Tracking Analysis (NTA)

For sizing and quantifying EVs, we employed a NanoSight particle tracking analyzer equipped with a 488 nm blue laser (NanoSight Ltd., Amesbury, United Kingdom). To achieve the optimal particle concentration our samples underwent a 1:10,000 dilution in 1 mL of ultrapure MiliPore water (Merck Milipore, Burlington, MA, USA). Video recordings were captured for 30 seconds in continuous infusion mode with 5 technical replicates. All procedures were performed as previously described [25].

We visually evaluated the acquired images and utilized NTA 3.4 NanoSight software (NanoSight Ltd., Amesbury, UK) for data processing. Background noise from all video data was automatically subtracted prior to particle tracking. Size distribution diagrams, mean values, and standard deviations were calculated using NTA 3.4 (NanoSight Ltd., Amesbury, UK) software and subsequently utilized for further analysis.

2.3 Cytokines

Plasma cytokine levels were assessed using a multiplex analysis platform and the MILLIPLEX® MAP Human Cytokine/Chemokine/Growth Factor Panel A (HCYTA-60K-PX48, MilliporeSigma, Burlington, MA, USA), as previously described [24,26]. In brief, the assay involved combining 25 µL of plasma samples with fluorescently labeled magnetic microsphere beads in the appropriate plate wells. This mixture was incubated overnight at +6 °C with agitation on a plate shaker. Detection antibodies were subsequently added and incubated for one hour at room temperature in the dark, followed by incubation with streptavidin-phycoerythrin under the same conditions. Standard samples were prepared according to the manufacturer's recommendations, and a calibration curve was generated for each detected cytokine. Results were acquired using the Luminex MAGPIX® (RUO) Instrument (Luminex, Austin, TX, USA). Data acquisition was performed using xPONENT software (v. 4.2) (Luminex Corporation, Austin, TX, USA) and analyzed with Milliplex Analyst 5.1 Flex software (Merck Milipore, Burlington, MA, USA). The panel of investigated cytokines is presented in **Supplementary Table 3**.

2.4 Statistics

Statistical analyses were performed using Statistica 7.0 (StatSoft, Oklahoma, OK, USA) and GraphPad Prism 8 (GraphPad Software Inc., San Diego, CA, USA). Data are presented as median and interquartile range (IQR). Group comparisons were conducted using ANOVA or Kruskal-Wallis tests, as appropriate, followed by Dunn's post-hoc test for pairwise comparisons. Mann-Whitney U tests were used to compare each group of patients with rejection to R0 recipients at corresponding time points. Statistical significance was defined as $p < 0.05$.

The LASSO (Least Absolute Shrinkage and Selection Operator) method, renowned for its ability to perform embedded feature selection via L1-regularization, was employed as a core filter to identify the most informative predictors from high-dimensional datasets [27]. Although LASSO is foundational to regression analysis, its core principle—imposing a penalty on the absolute magnitude of model coefficients—is directly applicable to linear models for classification when combined with an appropriate loss function (e.g., logistic loss). In this study, we leveraged this property for a multi-class classification task.

A defining characteristic of L1-regularization is its tendency to produce sparse solutions, driving the coefficients of less influential features to exactly zero. Thus, the model simultaneously performs classification and feature selection: features with non-zero coefficients are retained as relevant, while those with zero coefficients are effectively excluded. This provides an interpretable and parsimonious model.

All analyses were implemented in Python 3 using the scikit-learn library (v1.7.1) Python Software Foundation (Wilmington, DE, USA) [28]. To ensure simplicity and reproducibility in this initial feature screening phase, the regularization hyperparameter (λ, controlling the strength of

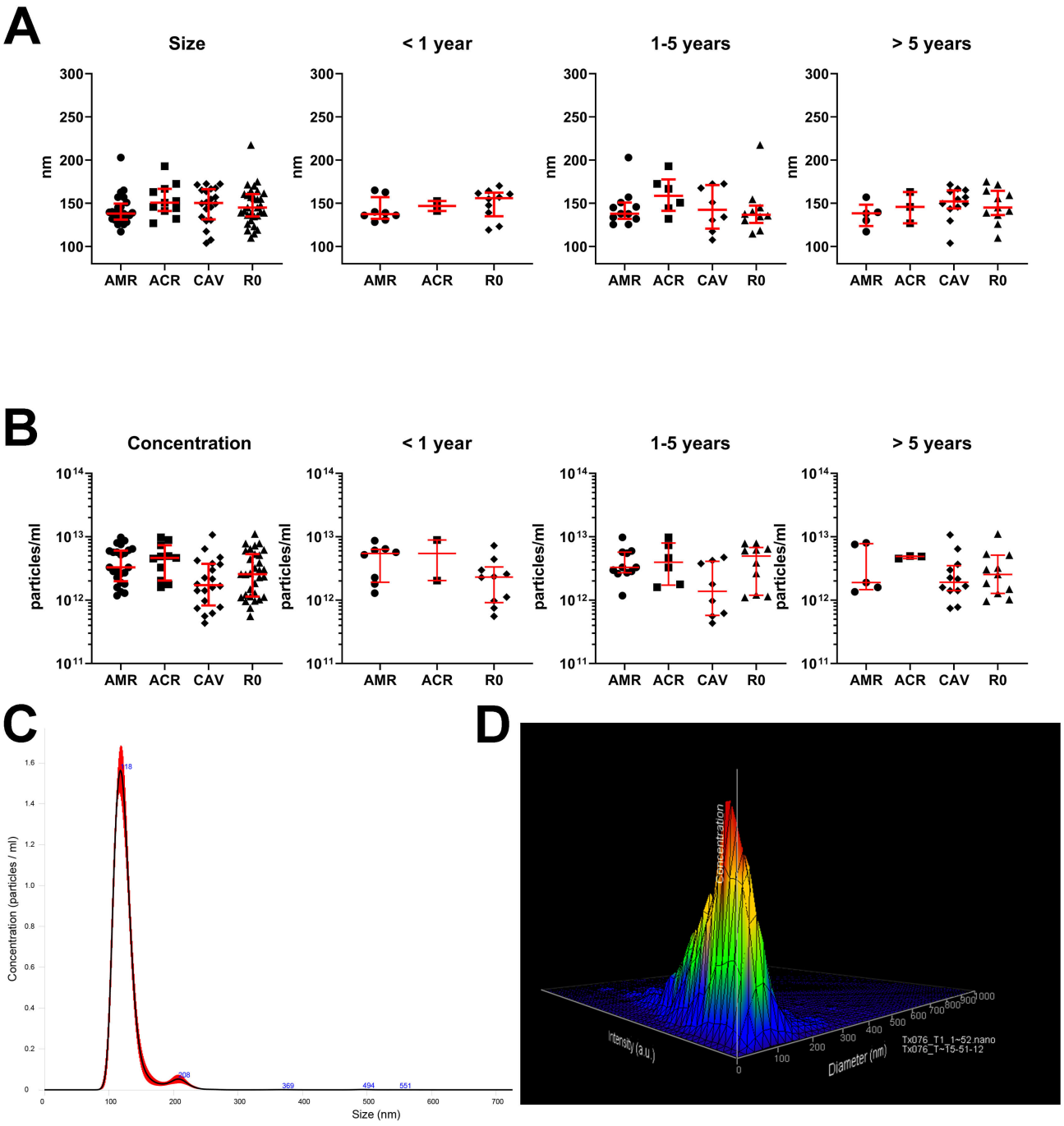

Fig. 1. Results of nanoparticle tracking analysis of samples within each time stratum (pooled sample results, <1 year, 1–5 years and >5 years post-transplantation). (A) Size. (B) Concentration. (C) Histogram of size distribution of representative sample. (D) 3D graph of size distribution (size vs. intensity vs. concentration) of representative sample.

the penalty) was fixed at 1.0, and all other parameters were kept at their library defaults.

The selection pipeline was applied independently to two biomarker categories: (1) a panel of unique patients for EVs, and (2) a panel of unique patients for cytokines. For each category, LASSO was run twice: once to discriminate by group and once by type of rejection. From each run, the top 15 features with the largest absolute coefficient magnitudes were selected. To ensure robustness and focus on consistently important biomarkers, only those features that appeared in both selection lists within their respective category (markers or cytokines) were retained for the subsequent stage of mutual Spearman correlation analysis.

3. Results

NTA revealed no differences in either the size or concentration of EVs in plasma of patients after HT within each

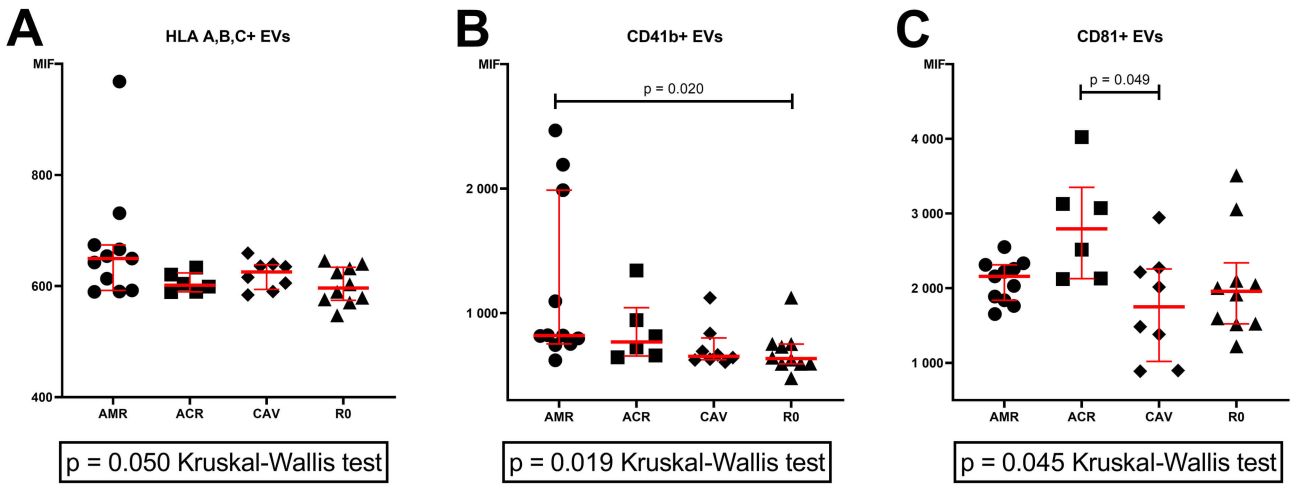

Fig. 2. Significant alterations in plasma extracellular vesicle (EV) populations observed 1–5 years following heart transplantation (HT). (A) Relative abundance of HLA A,B,C-positive EVs. (B) Relative abundance of CD41b-positive EVs. (C) Relative abundance of CD81-positive EVs. *Note.* Data were analyzed using the Kruskal-Wallis test, and Dunn's multiple comparisons test was performed to assess pairwise differences between groups.

time stratum (Fig. 1). Additionally, no differences according to the type of rejection were observed.

Analysis of EV phenotype in patients with and without heart transplant rejection revealed no significant differences when the transplantation time was not considered. Moreover, no differences in the EV profile were observed among patients without rejection within each stratum examined (less than 1 year, 1–5 years, and more than 5 years).

EV profiles showed no significant differences in the first year after transplantation in patients experiencing AMR, ACR, or in those without rejection (R0). A broader picture emerged between 1 and 5 years post-transplantation, with significant differences observed in all aforementioned groups and in recipients diagnosed with CAV (Fig. 2). Interestingly, this trend reversed after 5 years, with differences largely disappearing except for SSEA-4+ EVs, which exhibited significantly altered levels (p = 0.028) between groups at this later time point.

A critical observation is the time-dependent evolution of EV profiles in relation to the type of rejection experienced by the recipient. The dynamic changes observed in EVs from patients with AMR were particularly pronounced, revealing significant differences both across different time points post-transplantation and when compared to the relatively stable EV profiles of R0 recipients (Fig. 3).

Given the small number of patients with ACR and the uneven distribution of these patients across the different time points analyzed (n = 2, <1 year; n = 6, 1–5 years; n = 3, >5 years post-transplantation), we determined that any results derived from an analysis of temporal changes in EV profiles within this group would not be reliable or relevant.

Given the absence of CAV diagnoses in the first year post-transplantation, we focused our analysis on the 1–5 year and >5 year periods, comparing CAV patients to R0 controls at corresponding time points. These analyses revealed no significant differences in the temporal dynamics of EV profiles, nor were differences observed in direct comparisons to R0 patients.

Discriminant analysis effectively distinguished between different types of complications occurring within the first year after transplantation, based on the EV profiles (Fig. 4A). The most important variables in the model were EVs characterized by the presence of tetraspanins (CD9+ and CD63+) and platelet markers (CD62P+ and CD42a+), suggesting a role for these EVs in the early development of complications. Interestingly, the model also included EVs carrying markers associated with immune cell activity (CD49e+, CD25+, CD19+, CD1c+), indicating the involvement of immune-related processes.

The discriminant ability of the EV profile decreased over time, as indicated by an increase in Wilks' lambda to 0.15202 (Fig. 4B), suggesting a decline in the initial differences. However, this trend reversed after 5 years post-transplantation, with the increasing prevalence of CAV correlating with a renewed ability to discriminate between groups based on the EV profile (Fig. 4C). Despite the similarity between EV profiles in CAV and R0 patients, significant differences emerged in patients with AMR and ACR, both in comparison to each other and to the CAV/R0 groups. This corresponded with an increase in the number of EV markers associated with immune cell activity (CD3+, CD4+, CD49e+, CD86+, CD20+, CD14+, CD209+, CD1c+, CD29+).

We employed LASSO regression analysis as a feature selection step to identify the most relevant EVs and cytokines for subsequent correlation analysis. The relationships between these selected analytes were then assessed and are presented according to post-transplantation period

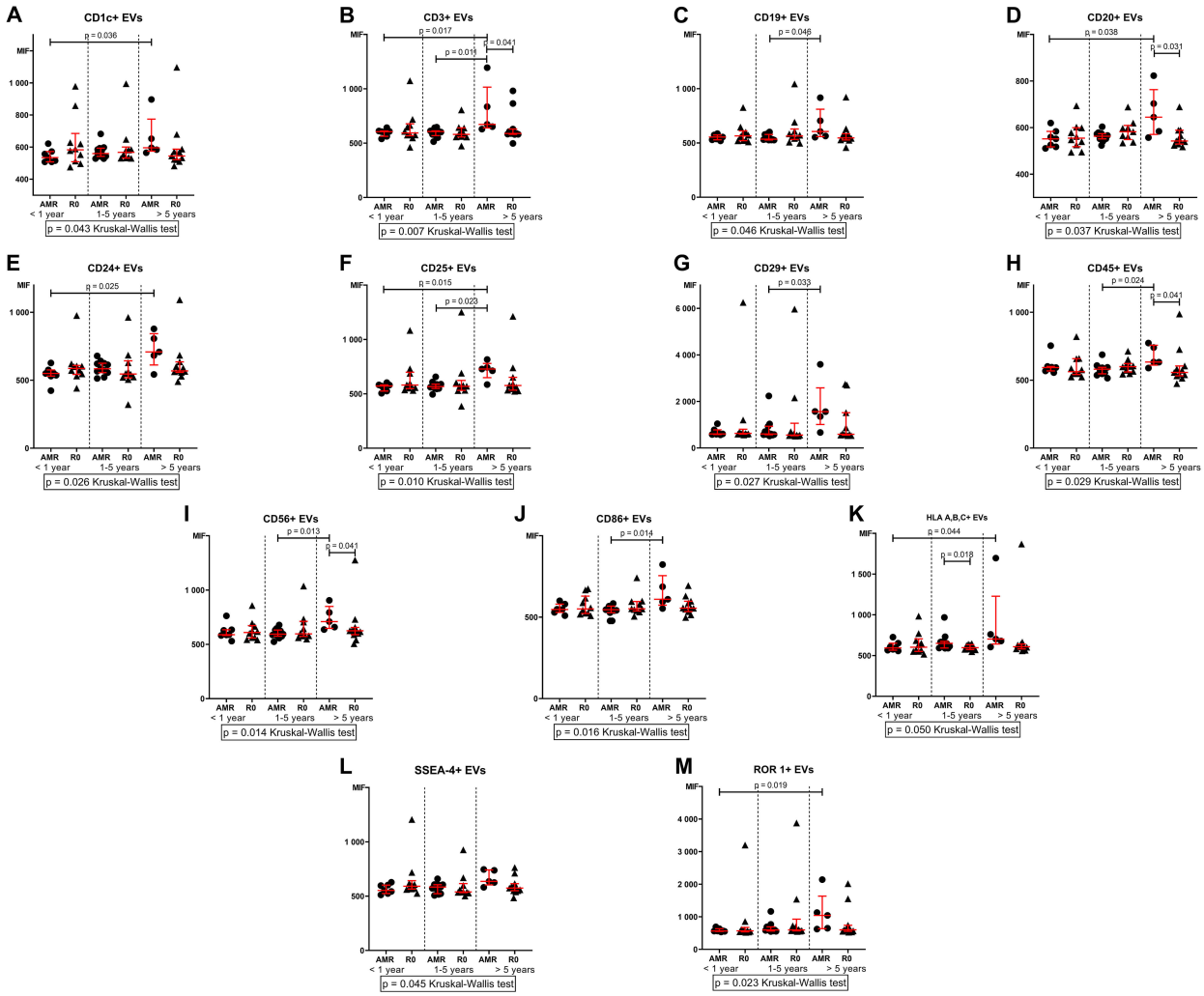

Fig. 3. Time-dependent alterations in plasma EV populations in AMR and R0 recipients. Relative abundance of: (A) CD1c+ EVs. (B) CD3+ EVs. (C) CD19+ EVs. (D) CD20+ EVs. (E) CD24+ EVs. (F) CD25+ EVs. (G) CD29+ EVs. (H) CD45+ EVs. (I) CD56+ EVs. (J) CD86+ EVs. (K) HLA A,B,C+ EVs. (L) SSEA-4+ EVs. (M) ROR 1+ EVs. *Note.* Kruskal-Wallis tests, followed by Dunn's post-hoc tests for pairwise comparisons, were used to assess differences between the AMR groups at each time point. Mann-Whitney U tests were used for paired comparisons with R0 recipients.

duration (Fig. 5A,D) and the type of rejection (Fig. 5B,E). Based on this analysis, we identified 10 cytokines and 11 EVs (Fig. 5C,F) that are most valuable in characterizing changes in cytokine and EV profiles according to post-transplantation duration and type of heart transplant rejection.

Taking into account the previously performed LASSO regression modeling, we then performed correlation analysis, identifying the most valuable associations between specific cytokines and EVs that are potentially specific for different types of heart transplant rejection. Correlation analysis of AMR patients (Fig. 6A) revealed distinct patterns in EV and cytokine relationships. Strong positive correlations were evident among EVs associated with immune cell activity (CD20+, CD19+, CD25+, CD86+), while cytokine correlations were less pronounced, primarily involving IL-22 and IL-17/IL-25. Notably, only correlations involving the latter cytokines extended to some EV populations.

Unlike the interconnected network observed in AMR patients, the correlation matrix for patients with ACR revealed a striking lack of significant associations between cytokine and EV levels (Fig. 6B). The correlation matrix for CAV patients (Fig. 6C) revealed a complex network of EV interactions, characterized by a high number of mostly weak correlations. Examining the cytokine compartment revealed that only IL-22 exhibited significant, albeit weak, correlations with specific EV populations. Interestingly, the remaining cytokines showed a striking lack of inter-correlations.

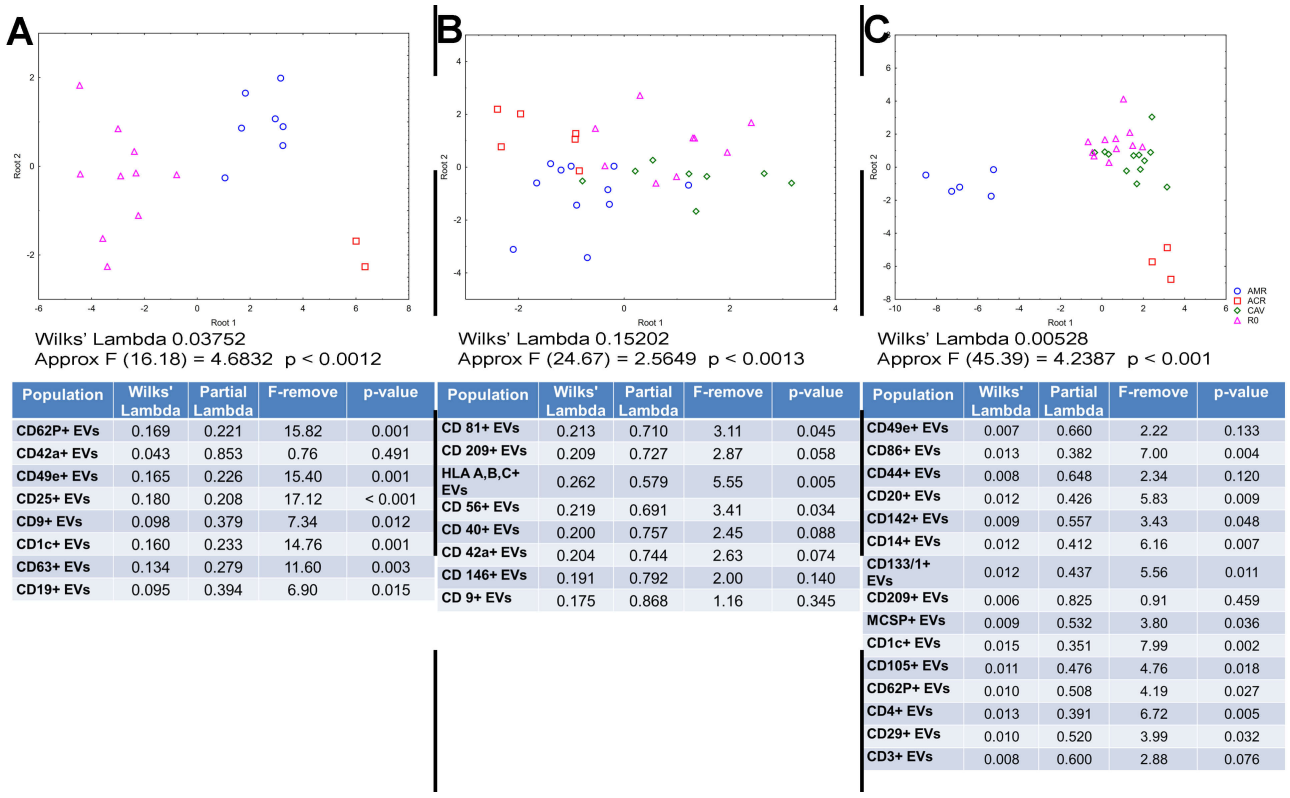

Population	Wilks' Lambda	Partial Lambda	F-remove	p-value
CD62P+ EVs	0.169	0.221	15.82	0.001
CD42a+ EVs	0.043	0.853	0.76	0.491
CD49e+ EVs	0.165	0.226	15.40	0.001
CD25+ EVs	0.180	0.208	17.12	< 0.001
CD9+ EVs	0.098	0.379	7.34	0.012
CD1c+ EVs	0.160	0.233	14.76	0.001
CD63+ EVs	0.134	0.279	11.60	0.003
CD19+ EVs	0.095	0.394	6.90	0.015

Population	Wilks' Lambda	Partial Lambda	F-remove	p-value
CD 81+ EVs	0.213	0.710	3.11	0.045
CD 209+ EVs	0.209	0.727	2.87	0.058
HLA A,B,C+ EVs	0.262	0.579	5.55	0.005
CD 56+ EVs	0.219	0.691	3.41	0.034
CD 40+ EVs	0.200	0.757	2.45	0.088
CD 42a+ EVs	0.204	0.744	2.63	0.074
CD 146+ EVs	0.191	0.792	2.00	0.140
CD 9+ EVs	0.175	0.868	1.16	0.345

Population	Wilks' Lambda	Partial Lambda	F-remove	p-value
CD49e+ EVs	0.007	0.660	2.22	0.133
CD86+ EVs	0.013	0.382	7.00	0.004
CD44+ EVs	0.008	0.648	2.34	0.120
CD20+ EVs	0.012	0.426	5.83	0.009
CD142+ EVs	0.009	0.557	3.43	0.048
CD14+ EVs	0.012	0.412	6.16	0.007
CD133/1+ EVs	0.012	0.437	5.56	0.011
CD209+ EVs	0.006	0.825	0.91	0.459
MCSP+ EVs	0.009	0.532	3.80	0.036
CD1c+ EVs	0.015	0.351	7.99	0.002
CD105+ EVs	0.011	0.476	4.76	0.018
CD62P+ EVs	0.010	0.508	4.19	0.027
CD4+ EVs	0.013	0.391	6.72	0.005
CD29+ EVs	0.010	0.520	3.99	0.032
CD3+ EVs	0.008	0.600	2.88	0.076

Fig. 4. Discriminant analysis revealed similarities and differences in EVs profile in patients with complications after heart transplantation (HT). (A) Less than 1 year after transplantation. (B) 1–5 years after transplantation. (C) More than 5 years after transplantation. AMR, antibody mediated rejection; ACR, acute cellular rejection; CAV, cardiac allograft vasculopathy; R0, without rejection.

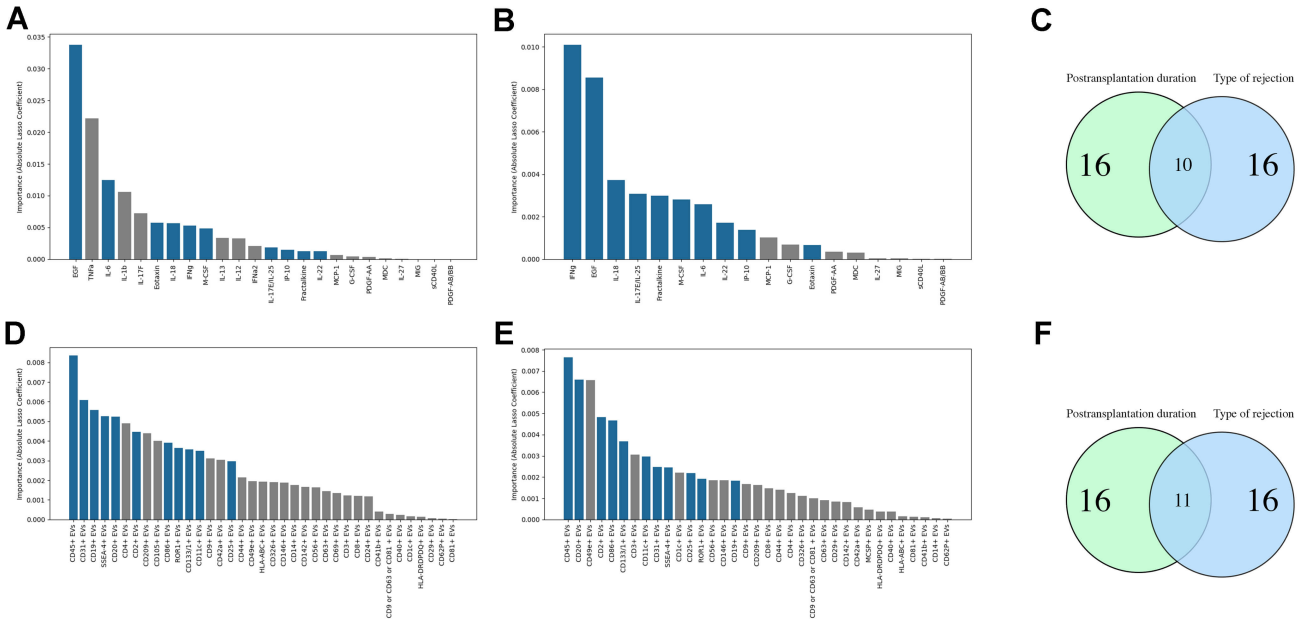

Fig. 5. Contribution of individual cytokines and EVs to Least Absolute Shrinkage and Selection Operator (LASSO) regression models predicting post-transplantation time and rejection type. (A,D) Significance of cytokines (A) and EVs (D) in the post-transplantation duration model. (B,E) Significance of cytokines (B) and EVs (E) in the rejection type model. (C,F) Venn diagrams showing common most significant cytokines (C) and EVs (F) in both models. Blue columns in subfigures (A,B,D,E) represent the parameters included in the subsequent analysis; grey columns represent the parameters excluded from the analysis.

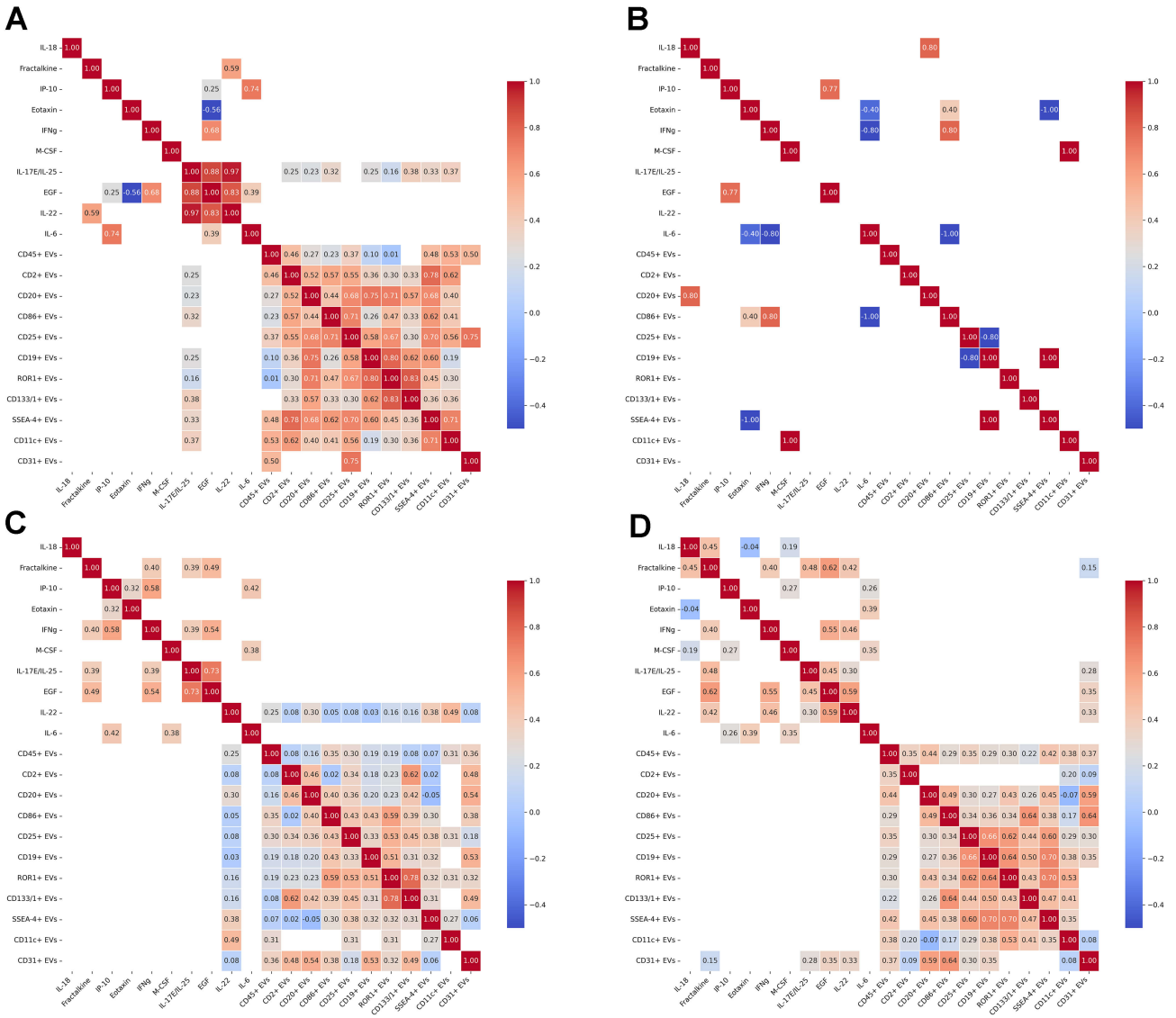

Fig. 6. Results of correlation analysis of cytokines and EVs, involved in predicting model by LASSO analysis. (A) Patients with AMR. (B) Patients with ACR. (C) Patients with CAV. (D) Patients with R0.

Unlike the patterns observed in AMR and CAV patients, R0 patients showed numerous positive correlations within the EV compartment but an almost complete absence of correlations between cytokines and EVs (Fig. 6D). Furthermore, cytokine levels were positively correlated with each other.

4. Discussion

Based on the obtained results, we propose that the EV profile in patients after HT varies according to the type of rejection and post-surgery duration. While we did not observe significant differences in individual EV types after the first year post-transplantation, we identified unique EV profiles (combinations of markers) characterizing AMR, ACR, and R0. The limited number of patients with ACR (n = 2) might limit the applicability of this finding to this specific type of rejection at this period. In contrast, Castellani et al. [29] investigated patients for 14 months post-HT and concluded that several EV subsets were significantly elevated in patients with both ACR and AMR compared to R0 (HLA-I, CD41b, ROR1, and SSEA-4). Furthermore, the expression levels of CD2+ and CD3+ EVs differed significantly between patients with ACR and R0. Moreover, EV expression of five well-established immunologic markers was significantly higher in patients with AMR than R0 [29]. Moreover, in a longitudinal study involving patients during the first year after HT, Burrello et al. [30] identified 14 differentially expressed EV antigens (CD2, CD3, CD4, CD8, CD19, CD20, CD24, CD25, CD45, CD49e, CD62P, CD142, CD209, HLA-I) that progressively increased in patients experiencing ACR from grade 1A/B to 3A [30]. The longitudinal design, with its valuable advantages, allowed the authors to reveal observations that led to the develop-

ment of a predictive model for non-invasive diagnosis of ACR in patients during the first year after HT [30].

In the next observation period, we identified notable variations in the levels of HLA-A,B,C+-, CD41b+-, and CD81+-expressing EVs among patients experiencing ACR, AMR, CAV, and those with R0 (Fig. 2). Interestingly, beyond the fifth year following transplantation, only the levels of EVs expressing SSEA-4 exhibited significant intergroup differences. These findings potentially indicate that the underlying pathogenic mechanisms of these rejection types diverge beyond the initial year post-transplant. Consequently, EVs displaying HLA class I molecules may contribute to the semi-direct presentation of donor antigens to T-cells by dendritic cells [7,17], thereby implicating EVs in the pathogenesis of ACR [31,32]. Besides, tetraspanins (CD37, CD53, CD63, CD81, and CD82) expressed on EVs released by B lymphocytes have also been suggested to participate in antigen presentation and pathogenesis of AMR [7,22]. Furthermore, vesicles from platelets, endothelial cells, monocytes, and leukocytes are involved in regulation of immune responses, inflammation, and coagulation that explains significant reaction of such EVs fractions as CD41b+ (platelet derived) [33,34].

In our study, EV profiles were compared only between AMR patients and the corresponding R0 group at each post-transplantation time stratum. All mentioned in Fig. 3 EVs showed significant differences across the three post-transplantation time strata in patients with AMR. Elevation of such types of EVs as HLA I+, CD45+, CD3+, and CD19+, associated with T- and B-cells, may correspond to participation of EVs in direct and in-direct antigen allorecognition increasing over the duration of post-transplantation period [7,35,36]. Moreover, levels of CD3+, CD20+, CD45+, and CD56+ EVs were increased in patients with AMR after 5 and more years after transplantation compared to recipients without rejection.

In contrast to prior reports, which showed reduced plasma levels of B-cell (CD19+) and T-cell (CD3+)-derived EVs in kidney transplant (KT) recipients experiencing AMR or allograft dysfunction (AD) compared to those with renal recovery [37], our study revealed an opposite pattern. We observed differences in the level of T- and B-cell-derived EVs across post-transplantation time strata. Notably, CD3+ EV levels in AMR patients more than 5 years post-transplant were significantly elevated compared to those without rejection ($p = 0.041$).

Prior studies analyzing the overall EV profile, rather than focusing on individual exosome populations, in heart transplant recipients have identified potential associations. Specifically, EVs expressing CD3, CD2, ROR1, SSEA-4, HLA-I, and CD41b distinguished R0 from ACR, while ROR1, SSEA-4, HLA-I, CD41b, HLA-II, CD326, CD19, CD25, and CD20 differentiated R0 from AMR patients [29]. However, this study did not investigate how these profiles change over time post-transplantation. Our hypothesis is that the interplay between the immune system and the transplanted organ is a dynamic process that unfolds differently at various stages post-transplant, with EVs serving as critical mediators of this temporal immune modulation.

Discriminant analysis revealed distinct EV profiles in patients with different types of transplanted heart rejection (ACR, AMR, CAV) and those with R0 (Fig. 3). Tetraspanins and platelet-derived EVs emerged as key discriminating factors during the first year post-transplantation, suggesting that inflammation and coagulation regulated by EVs are potentially leading factors in rejection pathogenesis. At later post-transplantation stages, the EV profile indicates an increased role for immune cells, as well as direct and indirect mechanisms of antigen presentation and immunity activation in the development of AMR and ACR. Notably, the EV profile of patients with CAV closely resembled that of patients with R0. This corresponds to previously published results indicating the role of EVs from B-cells in antigen presentation and donor-specific antibodies production [7]. Indeed, B-cells release high levels of EVs that carry MHC class I, MHC class II, CD45RA, components of the B-cell receptor (BCR), and tetraspanins, which are molecular features consistent with these functions [38]

EVs, including exosomes and microvesicles, play a crucial role in intercellular communication by transporting bioactive molecules, including cytokines [39]. Several studies highlight that EVs derived from different cell types carry distinct cytokine profiles, influencing immune responses and disease progression [14,40,41]. For instance, macrophage-derived exosomes contain IL-6 and IL-8 [42]. Recent studies demonstrate that immune cells secrete cytokines both in free-soluble forms and associated with EVs, with the distribution pattern depending primarily on the cellular origin rather than the cytokine type. For example, placental villous explants predominantly release cytokines like IL-2 and IL-4 in soluble form, while T-cells and monocytes secrete these same cytokines (along with CCL11, TGF-β, and TNF-α) primarily in EV-associated states—either encapsulated or surface-tethered. Cellular activation further modulates this balance, as stimuli such as LPS or poly(I:C) differentially alter EV sorting, shifting cytokines between soluble and EV-bound pools. *In vitro* studies demonstrated that cytokine-stimulated T-cells release IL-1β and TNF-α predominantly in EV-associated forms, with minimal free cytokine secretion [43]. Notably, EV-associated cytokines remain functional, though their mechanistic distinctions from free cytokines are increasingly explored [39,43,44,45].

Beyond simply carrying cytokines, EVs also actively modulate the production and release of cytokines by recipient cells, profoundly impacting immune responses [46]. One significant mechanism through which EVs regulate cytokine release involves their critical role in cell maturation. For instance, specific EVs have been demonstrated

to be essential for the maturation of plasmacytoid dendritic cells (pDCs). Upon stimulation by these EVs, mature pDCs were shown to upregulate the expression of pro-inflammatory cytokines such as IL-6 and IL-8, alongside co-stimulatory molecules. Extending this influence, these EV-stimulated pDCs subsequently exhibited the capacity to initiate the proliferation of allogeneic naive CD4+ T-cells, consequently triggering the secretion of key effector cytokines, including TNF-α and IFN-γ, from these T-cells. Importantly, this EV-dependent pDC maturation and its downstream effects were found to be specific to endothelial cell-derived EVs, highlighting the precise cellular origin requirement for such immunomodulatory roles, as EVs from platelets or lymphocytes failed to elicit comparable responses [47]. Human B cell exosomes can directly target T cells by delivery of specific antigens (i.e., allergens), thereby inducing T cell proliferation accompanied with Th2 cytokine synthesis (i.e., IL-5, IL-13) [48].

These diverse roles underscore the critical importance of simultaneously investigating EVs and cytokine levels (Fig. 6). The clinical relevance of EV-mediated cytokine modulation is further highlighted in conditions such as rejection following HT [49]. In such patients, distinct cytokine profiles were observed depending on the type of rejection. Significant, multiple correlations between cytokine levels were only noted in patients without rejection (R0). In contrast, patients with CAV and AMR exhibited only isolated correlational links in their cytokine levels. Interestingly, in patients with CAV, IL-22 levels significantly correlated with the levels of various relevant EV populations, suggesting a potential role for Th22 cells in this specific complication.

Furthermore, patients with AMR exhibited the most numerous and robust positive correlations in EVs levels. Conversely, in those with CAV, the strength of these associations was diminished, and in some instances, even negative. Specifically, the correlations between levels of various relevant EV populations were weaker compared to AMR, indicating differences in EVs involvement. In contrast, patients with ACR showed an absence of coordinated responses; no significant correlations were found between cytokine levels and EV levels, nor among the different EV populations themselves.

5. Limitations

The study employed a cross-sectional design. Although we analyzed patients across a broad range of post-transplantation time intervals (from 1 to 140 months) and included histologically verified rejection types (AMR, ACR, CAV), the absence of longitudinal follow-up with repeated measurements in the same individuals limits our ability to distinguish true temporal dynamics from inter-individual variability.

The study included patients with different types of rejection (AMR, ACR, CAV) and a control group without rejection (R0), but the sample sizes within certain subgroups, particularly when stratified by time post-transplantation, were relatively small. This may have limited statistical power for some comparisons.

6. Conclusions

Thus, circulating plasma EV profiles change over time in patients after HT. These profiles differ according to the type of transplant rejection, with the most pronounced differences observed one year or more after transplantation. EV levels were intercorrelated in the AMR, CAV and R0 groups, with the strongest positive correlations observed in AMR. Levels of the most prominent EV subpopulations correlated with IL-22 in patients with CAV, whereas in AMR they correlated with IL-17 and IL-25. These findings support the hypothesis that EVs may participate in both direct and indirect antigen presentation and in the regulation of immune responses leading to allograft rejection after HT.

Abbreviations

HT, heart transplantation; ACR, acute cellular rejection; AMR, antibody-mediated rejection; CAV, cardiac allograft vasculopathy; APC, antigen-presenting cell; EVs, extracellular vesicles; EMB, endomyocardial biopsy; ISHLT, International Society for Heart and Lung Transplantation; GCS, glucocorticosteroids; WBC, white blood cells; HDL, high density lipoproteins; LDL, low density lipoproteins; VLDL, very low density lipoproteins; LASSO, Least Absolute Shrinkage and Selection Operator; KT, kidney transplant; AD, allograft dysfunction; BCR, B-cell receptor; pDCs, plasmacytoid dendritic cells.

Availability of Data and Materials

The data that support the findings of this study are available from the corresponding author upon reasonable request.

Author Contributions

AA performed primary experiments and assisted with data analysis and methodology development. LK, MO, MB and MS curated patient data and collected and analysed clinical information. DS, EZ and OK collected samples and performed cytokine multiplex assays and their analysis. IG validated the results, performed statistical analysis, and contributed to writing the manuscript. IK co-supervised the project, secured funding, participated in experiments, and led manuscript writing and revision. AK and PF conceived and supervised the project, contributed substantially to study conception and design, and critically revised the manuscript. AG supervised the project, secured funding, conceptualized the study, performed primary experiments, analysed the data, and prepared the initial draft of the manuscript. All authors read and approved the final manuscript. All authors have participated sufficiently

in the work and agreed to be accountable for all aspects of the work. All authors contributed to editorial changes in the manuscript.

Ethics Approval and Consent to Participate

The study was conducted in accordance with the Declaration of Helsinki and was approved by the Institutional Ethics Committee of V.A. Almazov National Medical Research Centre (protocol code: №4101-22, date of approval 24 January 2022). All enrolled patients provided written informed consent.

Acknowledgment

The authors acknowledge the Research Equipment Sharing Center 'Preclinical Translational Research Centre' at Almazov National Medical Research Center for providing access to their facilities and resources.

Funding

This study was supported by a grant from the Russian Science Foundation (Grant №24-15-20016) and a grant from the St. Petersburg Science Foundation (Grant №24-15-20016).

Conflicts of Interest

The authors declare no conflicts of interest.

Declaration of AI and AI-Assisted Technologies in the Writing Process

During the preparation of this work the authors used ChatGpt-3 in order to check spell and grammar. After using this tool, the authors reviewed and edited the content as needed and takes full responsibility for the content of the publication.

Supplementary Material

Supplementary material associated with this article can be found, in the online version, at https://doi.org/10.31083/FBL50478.

References

[1] Heidenreich PA, Bozkurt B, Aguilar D, Allen LA, Byun JJ, Colvin MM, et al. 2022 AHA/ACC/HFSA Guideline for the Management of Heart Failure: A Report of the American College of Cardiology/American Heart Association Joint Committee on Clinical Practice Guidelines. Journal of the American College of Cardiology. 2022; 79: e263–e421. https://doi.org/10.1016/j.jacc.2021.12.012.

[2] Khush KK, Hsich E, Potena L, Cherikh WS, Chambers DC, Harhay MO, et al. The International Thoracic Organ Transplant Registry of the International Society for Heart and Lung Transplantation: Thirty-eighth adult heart transplantation report - 2021; Focus on recipient characteristics. The Journal of Heart and Lung Transplantation. 2021; 40: 1035–1049. https://doi.org/10.1016/j.healun.2021.07.015.

[3] Khush KK, Cherikh WS, Chambers DC, Harhay MO, Hayes D Jr, Hsich E, et al. The International Thoracic Organ Transplant Registry of the International Society for Heart and Lung Transplantation: Thirty-sixth adult heart transplantation report - 2019; focus theme: Donor and recipient size match. The Journal of Heart and Lung Transplantation. 2019; 38: 1056–1066. https://doi.org/10.1016/j.healun.2019.08.004.

[4] Pober JS, Chih S, Kobashigawa J, Madsen JC, Tellides G. Cardiac allograft vasculopathy: current review and future research directions. Cardiovascular Research. 2021; 117: 2624–2638. https://doi.org/10.1093/cvr/cvab259.

[5] Hagemeijer MC, van Oosterhout MFM, van Wichen DF, van Kuik J, Siera-de Koning E, Gmelig Meyling FHJ, et al. T cells in cardiac allograft vasculopathy are skewed to memory Th-1 cells in the presence of a distinct Th-2 population. American Journal of Transplantation. 2008; 8: 1040–1050. https://doi.org/10.1111/j.1600-6143.2008.02198.x.

[6] Hiemann NE, Meyer R, Wellnhofer E, Schoenemann C, Heidecke H, Lachmann N, et al. Non-HLA antibodies targeting vascular receptors enhance alloimmune response and microvasculopathy after heart transplantation. Transplantation. 2012; 94: 919–924. https://doi.org/10.1097/TP.0b013e3182692ad2.

[7] Gołębiewska JE, Wardowska A, Pietrowska M, Wojakowska A, Dębska-Ślizień A. Small Extracellular Vesicles in Transplant Rejection. Cells. 2021; 10: 2989. https://doi.org/10.3390/cells10112989.

[8] Chen Y, Heeger PS, Valujskikh A. In vivo helper functions of alloreactive memory CD4+ T cells remain intact despite donor-specific transfusion and anti-CD40 ligand therapy. Journal of Immunology. 2004; 172: 5456–5466. https://doi.org/10.4049/jimmunol.172.9.5456.

[9] Herrera OB, Golshayan D, Tibbott R, Salcido Ochoa F, James MJ, Marelli-Berg FM, et al. A novel pathway of alloantigen presentation by dendritic cells. Journal of Immunology. 2004; 173: 4828–4837. https://doi.org/10.4049/jimmunol.173.8.4828.

[10] Aquino A, Rubinstein A, Kudryavtsev I, Yakovlev A, Golovkin A. Extracellular vesicles as the drug delivery vehicle for gene-based therapy. Applied Physics Reviews. 2025; 12: 041301. https://doi.org/10.1063/5.0255519.

[11] Chang WH, Cerione RA, Antonyak MA. Extracellular Vesicles and Their Roles in Cancer Progression. Methods in Molecular Biology. 2021; 2174: 143–170. https://doi.org/10.1007/978-1-0716-0759-6_10.

[12] Colombo M, Raposo G, Théry C. Biogenesis, secretion, and intercellular interactions of exosomes and other extracellular vesicles. Annual Review of Cell and Developmental Biology. 2014; 30: 255–289. https://doi.org/10.1146/annurev-cellbio-101512-122326.

[13] Fedorov A, Kondratov K, Kishenko V, Mikhailovskii V, Kudryavtsev I, Belyakova M, et al. Application of high-sensitivity flow cytometry in combination with low-voltage scanning electron microscopy for characterization of nanosized objects during platelet concentrate storage. Platelets. 2020; 31: 226–235. https://doi.org/10.1080/09537104.2019.1599337.

[14] Buzas EI. The roles of extracellular vesicles in the immune system. Nature Reviews. Immunology. 2023; 23: 236–250. https://doi.org/10.1038/s41577-022-00763-8.

[15] Marino J, Babiker-Mohamed MH, Crosby-Bertorini P, Paster JT, LeGuern C, Germana S, et al. Donor exosomes rather than passenger leukocytes initiate alloreactive T cell responses after transplantation. Science Immunology. 2016; 1: aaf8759. https://doi.org/10.1126/sciimmunol.aaf8759.

[16] Muller E. Donor Dendritic Cell-Derived Exosomes Promote Allograft-Targeting Immune Response. Transplantation. 2016; 100: 2237–2238.

[17] Morelli AE, Bracamonte-Baran W, Burlingham WJ. Donor-derived exosomes: the trick behind the semidirect pathway of al-

lorecognition. Current Opinion in Organ Transplantation. 2017; 22: 46–54. https://doi.org/10.1097/MOT.0000000000000372.

[18] Dieudé M, Bell C, Turgeon J, Beillevaire D, Pomerleau L, Yang B, et al. The 20S proteasome core, active within apoptotic exosome-like vesicles, induces autoantibody production and accelerates rejection. Science Translational Medicine. 2015; 7: 318ra200. https://doi.org/10.1126/scitranslmed.aac9816.

[19] Wiebe C, Gibson IW, Blydt-Hansen TD, Pochinco D, Birk PE, Ho J, et al. Rates and determinants of progression to graft failure in kidney allograft recipients with de novo donor-specific antibody. American Journal of Transplantation. 2015; 15: 2921–2930. https://doi.org/10.1111/ajt.13347.

[20] Chong AS. B cells as antigen-presenting cells in transplantation rejection and tolerance. Cellular Immunology. 2020; 349: 104061. https://doi.org/10.1016/j.cellimm.2020.104061.

[21] Raposo G, Nijman HW, Stoorvogel W, Liejendekker R, Harding CV, Melief CJ, et al. B lymphocytes secrete antigen-presenting vesicles. The Journal of Experimental Medicine. 1996; 183: 1161–1172. https://doi.org/10.1084/jem.183.3.1161.

[22] Escola JM, Kleijmeer MJ, Stoorvogel W, Griffith JM, Yoshie O, Geuze HJ. Selective enrichment of tetraspan proteins on the internal vesicles of multivesicular endosomes and on exosomes secreted by human B-lymphocytes. The Journal of Biological Chemistry. 1998; 273: 20121–20127. https://doi.org/10.1074/jbc.273.32.20121.

[23] Kondratov K, Nikitin Y, Fedorov A, Kostareva A, Mikhailovskii V, Isakov D, et al. Heterogeneity of the nucleic acid repertoire of plasma extracellular vesicles demonstrated using high-sensitivity fluorescence-activated sorting. Journal of Extracellular Vesicles. 2020; 9: 1743139. https://doi.org/10.1080/20013078.2020.1743139.

[24] Aquino A, Abutalimova N, Ma Y, Ismail-Zade I, Grebennik V, Rubinstein A, et al. Differences in Plasma Extracellular Vesicles of Different Origin in On-Pump Versus Off-Pump Cardiac Surgery. Current Issues in Molecular Biology. 2024; 46: 13058–13077. https://doi.org/10.3390/cimb46110779.

[25] Petrova T, Kalinina O, Aquino A, Grigoryev E, Dubashynskaya NV, Zubkova K, et al. Topographic Distribution of miRNAs (miR-30a, miR-223, miR-let-7a, miR-let-7f, miR-451, and miR-486) in the Plasma Extracellular Vesicles. Non-Coding RNA. 2024; 10: 15. https://doi.org/10.3390/ncrna10010015.

[26] Kalinina O, Golovkin A, Zaikova E, Aquino A, Bezrukikh V, Melnik O, et al. Cytokine Storm Signature in Patients with Moderate and Severe COVID-19. International Journal of Molecular Sciences. 2022; 23: 8879. https://doi.org/10.3390/ijms23168879.

[27] Tibshirani R. Regression Shrinkage and Selection via the Lasso. Journal of the Royal Statistical Society Series B: Statistical Methodology. 1996; 58: 267–288. https://doi.org/10.1111/j.2517-6161.1996.tb02080.x.

[28] Pedregosa F, Varoquaux G, Gramfort A, Michel V, Thirion B, Grisel O, et al. Scikit-learn: Machine Learning in Python. Journal of Machine Learning Research. 2011; 12: 2825–2830.

[29] Castellani C, Burrello J, Fedrigo M, Burrello A, Bolis S, Di Silvestre D, et al. Circulating extracellular vesicles as non-invasive biomarker of rejection in heart transplant. The Journal of Heart and Lung Transplantation. 2020; 39: 1136–1148. https://doi.org/10.1016/j.healun.2020.06.011.

[30] Burrello J, Panella S, Barison I, Castellani C, Burrello A, Airale L, et al. Machine learning-assisted assessment of extracellular vesicles can monitor cellular rejection after heart transplant. Communications Medicine. 2025; 5: 288. https://doi.org/10.1038/s43856-025-00999-0.

[31] Mirzakhani M, Shahbazi M, Oliaei F, Mohammadnia-Afrouzi M. Immunological biomarkers of tolerance in human kidney transplantation: An updated literature review. Journal of Cellular Physiology. 2019; 234: 5762–5774. https://doi.org/10.1002/jcp.27480.

[32] Benichou G, Valujskikh A, Heeger PS. Contributions of direct and indirect T cell alloreactivity during allograft rejection in mice. Journal of Immunology. 1999; 162: 352–358.

[33] Giarraputo A, Barison I, Fedrigo M, Burrello J, Castellani C, Tona F, et al. A Changing Paradigm in Heart Transplantation: An Integrative Approach for Invasive and Non-Invasive Allograft Rejection Monitoring. Biomolecules. 2021; 11: 201. https://doi.org/10.3390/biom11020201.

[34] Li Y, He X, Li Q, Lai H, Zhang H, Hu Z, et al. EV-origin: Enumerating the tissue-cellular origin of circulating extracellular vesicles using exLR profile. Computational and Structural Biotechnology Journal. 2020; 18: 2851–2859. https://doi.org/10.1016/j.csbj.2020.10.002.

[35] Ravichandran R, Bansal S, Rahman M, Sureshbabu A, Sankpal N, Fleming T, et al. Extracellular Vesicles Mediate Immune Responses to Tissue-Associated Self-Antigens: Role in Solid Organ Transplantations. Frontiers in Immunology. 2022; 13: 861583. https://doi.org/10.3389/fimmu.2022.861583.

[36] Korutla L, Hu R, Liu Y, Romano C, Habertheuer A, Abedi P, et al. Circulating Tissue Specific Extracellular Vesicles for Noninvasive Monitoring of Acute Cellular Rejection in Clinical Heart Transplantation. Transplantation. 2025; 109: 1540–1550. https://doi.org/10.1097/TP.0000000000005369.

[37] Jacob V, de Berny Q, Brazier F, Presne C, Lion J, Ouled-Haddou H, et al. Quantification of Urine and Plasma Levels of Extracellular Vesicles in a Cohort of Kidney Transplant Recipients and Chronic Kidney Disease Patients. International Journal of Molecular Sciences. 2025; 26: 3635. https://doi.org/10.3390/ijms26083635.

[38] Saunderson SC, Schuberth PC, Dunn AC, Miller L, Hock BD, MacKay PA, et al. Induction of exosome release in primary B cells stimulated via CD40 and the IL-4 receptor. Journal of Immunology. 2008; 180: 8146–8152. https://doi.org/10.4049/jimmunol.180.12.8146.

[39] Aiello A, Giannessi F, Percario ZA, Affabris E. An emerging interplay between extracellular vesicles and cytokines. Cytokine & Growth Factor Reviews. 2020; 51: 49–60. https://doi.org/10.1016/j.cytogfr.2019.12.003.

[40] Hazrati A, Soudi S, Malekpour K, Mahmoudi M, Rahimi A, Hashemi SM, et al. Immune cells-derived exosomes function as a double-edged sword: role in disease progression and their therapeutic applications. Biomarker Research. 2022; 10: 30. https://doi.org/10.1186/s40364-022-00374-4.

[41] Xu MY, Ye ZS, Song XT, Huang RC. Differences in the cargos and functions of exosomes derived from six cardiac cell types: a systematic review. Stem Cell Research & Therapy. 2019; 10: 194. https://doi.org/10.1186/s13287-019-1297-7.

[42] Holder B, Jones T, Sancho Shimizu V, Rice TF, Donaldson B, Bouqueau M, et al. Macrophage Exosomes Induce Placental Inflammatory Cytokines: A Novel Mode of Maternal-Placental Messaging. Traffic. 2016; 17: 168–178. https://doi.org/10.1111/tra.12352.

[43] Fitzgerald W, Freeman ML, Lederman MM, Vasilieva E, Romero R, Margolis L. A System of Cytokines Encapsulated in ExtraCellular Vesicles. Scientific Reports. 2018; 8: 8973. https://doi.org/10.1038/s41598-018-27190-x.

[44] Hussain MT, Iqbal AJ, Norling LV. The Role and Impact of Extracellular Vesicles in the Modulation and Delivery of Cytokines during Autoimmunity. International Journal of Molecular Sciences. 2020; 21: 7096. https://doi.org/10.3390/ijms21197096.

[45] Stow JL, Murray RZ. Intracellular trafficking and secretion of inflammatory cytokines. Cytokine & Growth Factor Reviews. 2013; 24: 227–239. https://doi.org/10.1016/j.cytogfr.2013.04.001.

[46] Yáñez-Mó M, Siljander PRM, Andreu Z, Zavec AB, Borràs FE, Buzas EI, et al. Biological properties of extracellular vesicles and their physiological functions. Journal of Extracellular Vesicles. 2015; 4: 27066. https://doi.org/10.3402/jev.v4.27066.

[47] Angelot F, Seillès E, Biichlé S, Berda Y, Gaugler B, Plumas J, et al. Endothelial cell-derived microparticles induce plasmacytoid dendritic cell maturation: potential implications in inflammatory diseases. Haematologica. 2009; 94: 1502–1512. https://doi.org/10.3324/haematol.2009.010934.

[48] Admyre C, Bohle B, Johansson SM, Focke-Tejkl M, Valenta R, Scheynius A, et al. B cell-derived exosomes can present allergen peptides and activate allergen-specific T cells to proliferate and produce TH2-like cytokines. The Journal of Allergy and Clinical Immunology. 2007; 120: 1418–1424. https://doi.org/10.1016/j.jaci.2007.06.040.

[49] Korneva L, Sazonova Y, Bortsova M, Simonenko M, Baratashvili G, Kalinina O, et al. Successful Experience of Managing Resistant Antibody-Mediated Cardiac Allograft Rejection with Extracorporeal Photopheresis. Transplantology. 2025; 6: 29. https://doi.org/10.3390/transplantology6040029.